

Micro-electromagnets for atom manipulation

M. Drndić, K. S. Johnson,^{a)} J. H. Thywissen, M. Prentiss, and R. M. Westervelt^{b)}
Department of Physics, Harvard University, Cambridge, Massachusetts 02138

(Received 2 October 1997; accepted for publication 30 March 1998)

Micro-electromagnets for atom manipulation have been constructed, including magnetic mirrors (serpentine patterns) and traps (circular patterns). They consist of planar micron-scale Au wires on sapphire substrates fabricated using lithography and electroplating. At liquid nitrogen or helium temperatures in vacuum the wires support currents of several amperes with current density $\sim 10^8$ A/cm² and power dissipation ~ 10 kW/cm², and they produce magnetic fields to 0.3 T and gradients to 10^3 T/cm. The micro-electromagnet mirror was used to deflect a beam of metastable helium atoms at grazing angles ~ 0.5 mrad. © 1998 American Institute of Physics.
 [S0003-6951(98)00822-5]

Recent progress in atom optics was stimulated by advances in laser cooling and microfabrication. Light-atom interactions were used to demonstrate deflection, diffraction, focusing, and trapping of atoms,¹ while microfabrication techniques were used to construct structures with small enough periods to diffract thermal atom beams.^{1,2} Similarly, advances have taken place in the use of magnetic field gradients in novel manipulation schemes such as mirrors, gratings, traps,³ and lenses.⁴ Specifically, mirrors for atoms have been proposed⁵ and demonstrated using macroscopic permanent rare-earth magnets,⁶ microscopic magnetic tapes,⁷ and magnetized floppy disks.⁸ Recently, the use of microscopic planar geometries for small scale atomic traps has been proposed.⁹

In this letter we describe the fabrication, properties and testing of micro-electromagnets for atom manipulation. Specifically, we describe the use of a micro-electromagnet mirror to deflect a thermal beam of metastable helium (He*) atoms. The micro-electromagnets consist of planar micron-scale Au wires on sapphire substrates fabricated using photolithography and electroplating. Photolithography allows for the fabrication of complex patterns across large surface areas with excellent control to create novel field configurations for atom manipulation. Electroplating permits high currents (current density of $\sim 10^8$ A/cm², power dissipation ~ 10 kW/cm²) and magnetic fields to $B \sim 0.3$ T with gradients $|\nabla B| \sim 10^3$ T/cm. We present mirrors (serpentine pattern) and traps (circular patterns) for atoms. These devices have several advantages. The magnetic field is tunable, and time-dependent potentials¹⁰ can be realized. Substrates with excellent surface smoothness are widely available. The effect of any wire irregularities is suppressed by Kirchoff's current law which ensures that the same current flows throughout the electromagnet. Micro-traps could be used for studies of small numbers of cold atoms confined to regions with dimensions comparable to the de Broglie wavelength. We can fabricate arrays of large numbers of traps, as well as a nested series of traps. Such structures could be used to capture atoms in a

large volume and then compress them to a much smaller volume.⁹

Magnetic fields B , gradients $|\nabla B|$, and curvatures $\nabla^2 B$ generated from current carrying wires typically scale as $B \propto I/d$, $|\nabla B| \propto I/d^2$, and $\nabla^2 B \propto I/d^3$, where I is the wire current and d is the characteristic size of the system. The maximum current is limited by ohmic heating to values $I_{\max} \propto d$, such that B is independent of size, while $|\nabla B| \propto 1/d$ and $\nabla^2 B \propto 1/d^2$ are size dependent. Thus, micro-electromagnets can produce the same fields but larger gradients than macroscopic electromagnets, resulting in stronger forces for the confinement of atoms. If we consider a normal wire of width w on a planar substrate carrying a current I , the condition to remove the ohmic heating via heat conduction through the substrate gives $I/w \leq (\kappa \Delta T_{\max} / \rho)^{1/2}$, where κ is the thermal conductivity of the wire, ρ is the electrical resistivity, and ΔT_{\max} is the maximum allowable temperature difference to the substrate. For Au at room temperature with $\Delta T_{\max} = 100$ K and standard values for κ and ρ ,¹¹ we have $I/w \leq 1 \times 10^4$ A/cm. Cooling can be used to achieve even higher values of I/w by reducing ρ and increasing κ . We have experimentally investigated Au, Cu, and Ag wires on sapphire substrates. The best results are obtained with Au, for which we achieved current densities $\sim 10^8$ A/cm² (see below).

Superconducting devices made of Nb on Si substrates were also fabricated to investigate their current-carrying capabilities. Current densities up to $\sim 2.5 \times 10^6$ A/cm² were achieved at 4.2 K. The maximum current in superconductors is limited either by the critical field (type I) or by flux pinning (type II).¹² Among existing materials, Nb, NbTi, and Nb₃Sn could be used to obtain current densities up to 10^7 A/cm²,¹² which is still lower than the values we report for Au.

The interaction of atoms with magnetic fields for atom optics has been studied in detail.^{3,9} The manipulation of neutral atoms using current carrying wires is based on the Zeeman interaction between an inhomogeneous magnetic field and the atomic magnetic dipole moment. This interaction avoids spontaneous emission which occurs in atom-optical elements based on light-atom interactions. If the magnetic moment can follow the local magnetic field, the motion is adiabatic and the external field affects only the center of

^{a)}Present address: IGEN International, Inc., 16020 Industrial Drive, Gaithersburg, MD 20877.

^{b)}Electronic mail: westervelt@deas.harvard.edu

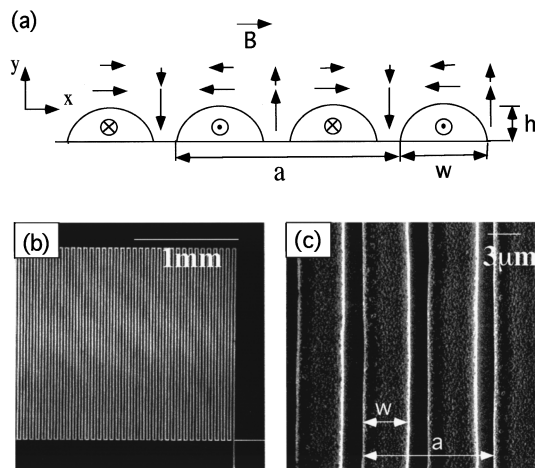


FIG. 1. (a) Schematic diagram of a serpentine micro-electromagnet mirror and the magnetic field above it, a is the period, w the wire width, and h the wire height; (b) and (c) scanning electron microscope (SEM) images of Au mirrors on sapphire substrates: (b) $a=48 \mu\text{m}$, $w=12 \mu\text{m}$, $h=0.3 \mu\text{m}$; (c) $a=12 \mu\text{m}$, $w=4.3 \mu\text{m}$, $h=0.9 \mu\text{m}$.

mass motion. Consequently, the gradient force due to the magnetic field is $\mathbf{F}=\nabla(\boldsymbol{\mu}\cdot\mathbf{B})=-g_F m_F \mu_B \nabla B$, where μ_B is the Bohr magneton, g_F is the Lande g factor, and m_F is the magnetic quantum number of the atomic substrate.

Figure 1 shows a magnetic mirror for atoms using a serpentine pattern of current-carrying wires. The magnitude B of the magnetic field decays exponentially in the direction perpendicular to the mirror plane, with characteristic length $k^{-1}=a/2\pi$, where a is the period [see Fig. 1(a)]. At distances $y \gg a/2\pi$, the amplitude is $B(x,y)=B_0 e^{-ky}(1+\alpha e^{-2ky} \cos 2kx+\dots)$, where y is the perpendicular distance from the mirror surface, x is the distance along the mirror perpendicular to the wires, and $\alpha(0 \leq \alpha \leq 1)$ is a coefficient determined by the boundary conditions.¹³ Figures 1(b) and 1(c) are scanning electron microscope images of fabricated micro-electromagnet mirrors. We have made mirrors with periods [a in Fig. 1(a)] ranging from $a=12 \mu\text{m}$ to $a=200 \mu\text{m}$, covering areas up to 1 cm^2 . The fabrication is done in two steps: lithography and electroplating. First, photolithography is used to define the wire geometry on a 0.5 mm thick sapphire substrate 2.5 cm in diameter. We evaporate a 1000–4000 Å thick layer of Au on top of a 50 Å Cr adhesion layer. The wire is then electroplated with Au using In contacts and Cu leads to further reduce the resistance. Plating is done using a sodium gold sulfite solution in H_2O (3% $\text{Na}_3\text{Au}(\text{SO}_3)_2$, 8% Na_2SO_3) at 60 C with Pt or Au anodes¹⁴ at low currents ($<1 \text{ mA}$) to obtain smooth surfaces. Using Faraday's law $M=KQ$, where M is the deposited mass, K is the material constant ($K=2 \times 10^{-3} \text{ g/C}$ for gold), and Q is the required charge, we estimate Q to grow the wires to desired sizes.

Using the same procedure described above, we have fabricated other wire patterns for atom manipulation. Figures 2(a), 2(b), and 2(c) show scanning electron microscope images of micro-electromagnet traps as suggested theoretically by Weinstein *et al.*⁹ The radii of the circular traps vary from 30 to 50 μm with wire width $w=3 \mu\text{m}$. We have also fabricated arrays of traps as shown in Fig. 2(d).

Micro-electromagnets were tested in vacuum at cryo-

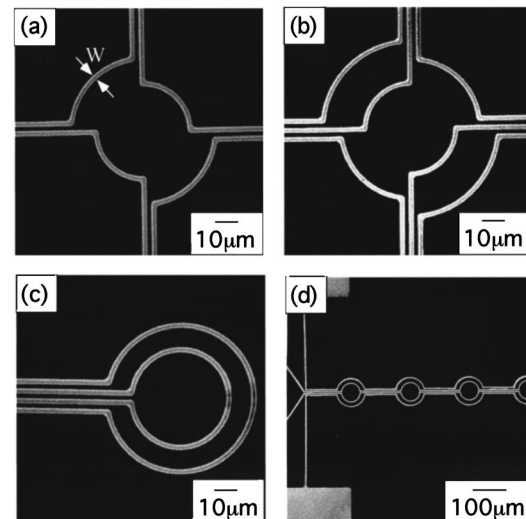


FIG. 2. SEM images of micro-electromagnets with geometries suggested (see Ref. 9) for trapping atoms. Traps are Au on sapphire substrates with $w=3 \mu\text{m}$ and $h=1 \mu\text{m}$: (a) two half loops, (b) three concentric half loops, (c) two full loops, (d) array of traps.

genic temperatures in an atomic beam apparatus. The sapphire substrate was tightly clamped to the end of a copper cold finger 0.5 m long and 1 cm in diameter, and heat sunk to liquid He in a Precision Cryogenics Dewar. The copper current leads were thermally anchored to the cold finger. An outer copper shield extending from the liquid N_2 bath of the Dewar was used to shield the inner cold finger from black-body radiation. The position of micro-electromagnets with respect to the beam was controlled by a set of manipulators to μm -scale precision. The substrate temperature T_s was monitored with a Si diode thermometer; for liquid He cooling $T_s=17 \text{ K}$ and for liquid N_2 $T_s=96 \text{ K}$. A pulse generator and programmable power supply with output up to 60 V at 20 A was used to energize the devices.

Figure 3(a) shows measured current–voltage (I – V) curves and computed fields B at the surface of the wires obtained for a micro-electromagnet mirror. The mirror characteristics are area $2 \times 2 \text{ mm}^2$, period $a=48 \mu\text{m}$, wire width $w=20 \mu\text{m}$, and thickness $h=3 \mu\text{m}$. Voltage pulses were applied to the mirror with low duty cycles ($<5\%$) at 300, 100, and 20 K. As shown, mirror currents up to $I=3 \text{ A}$ were achieved at 20 K using 1% duty cycle pulses. The surface field B was estimated assuming a rectangular wire $3 \times 20 \mu\text{m}^2$ with uniform current density. For $I=3 \text{ A}$ this gives $B \sim 0.1 \text{ T}$, sufficient to reflect 300 K thermal atoms

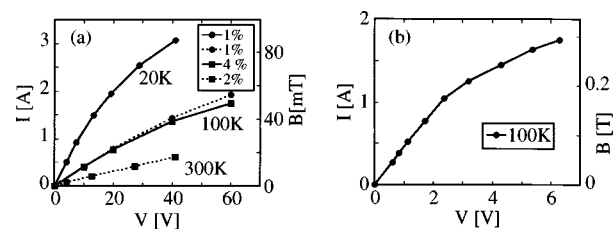


FIG. 3. (a) Measured I – V characteristics and computed fields B at the wire surface for a micro-electromagnet mirror at 300, 100, and 20 K pulsed at low duty cycle as indicated; mirror area $2 \times 2 \text{ mm}^2$, $a=48 \mu\text{m}$, $w=20 \mu\text{m}$, $h=3 \mu\text{m}$, and inductance $L=0.05 \mu\text{H}$. (b) Measured trap I – V characteristics and computed field B at the wire surface at 100 K for dc excitation; the device is shown in Fig. 2(a).

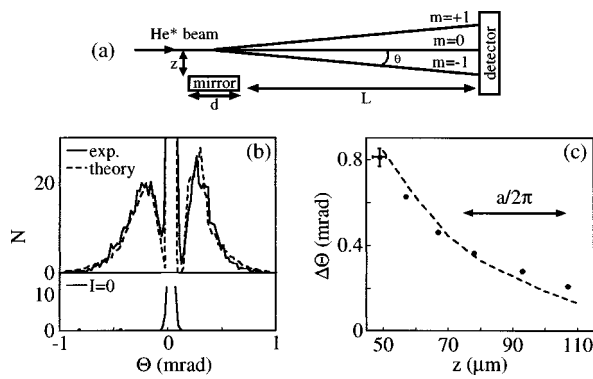


FIG. 4. (a) Schematic diagram of the experimental setup used to deflect He^* atoms with a micro-electromagnet mirror; $L=1.6$ m, $d=1$ cm. (b) The spatial distribution of deflected atoms after interacting with the mirror field at $I=1.04$ A and $I=0$. Solid line is the raw experimental data; dashed line is a numerical calculation which assumes an exponentially decaying field. (c) Angular splitting $\Delta\theta$ of He^* atoms as a function of the atom-mirror separation z . Dots are experimental measurements; dashed line is a numerical calculation. Representative error bars are shown.

grazing angles and colder atoms at arbitrary angles.

Figure 3(b) shows dc I - V characteristics and the corresponding surface field B obtained at 100 K for the micro-electromagnet trap shown in Fig. 2(a) with $w=3$ μm and $h=1$ μm . As shown this device can carry a constant current of $I=1.8$ A, which corresponds to $B\cong 0.3$ T, and the field gradient at the surface $|\nabla B|\sim 10^3$ T/cm.

To test the micro-electromagnet mirror and to probe the field above it, the beam of He^* atoms¹⁵ (in the 2^3S_1 state, $J=1$, $m_J=0, \pm 1$) was deflected by the mirror field as schematically illustrated in Fig. 4(a). The mean velocity of the He^* beam is $v\sim 1800$ m/s. The beam was deflected by a micro-electromagnet mirror with area 0.5×1 cm^2 , $a=200$ μm , $w=91$ μm , and $h=12$ μm and detected by a micro-channel plate located a distance $L=1.6$ m from the mirror [see Fig. 4(a)]. The beam was incident parallel to the mirror plane and parallel to the wires in the array to assure adiabaticity.

Figure 4(b) shows the spatial distribution of He^* atoms detected after interacting with the mirror carrying a current $I=1.04$ A (top) and $I=0$ (bottom). The separation between the center of the beam and the mirror is $z=58\pm 3$ μm . As shown, three peaks arise when the mirror is on: the central peak from the undeflected atoms ($m_J=0$ state), the right peak from the repelled atoms ($m_J=1$ state), and the left peak from the attracted atoms ($m_J=-1$ state). The asymmetry in the peaks results from a lensing effect due to opposite cur-

vature of the potentials responsible for the deflection.¹⁰ Figure 4(c) shows how the angular separation between the $m=\pm 1$ peaks, $\Delta\theta$, varies with mirror position z (and magnetic field) for fixed current $I=1.38$ A. The dashed line, a numerical calculation of $\Delta\theta$ which assumes an exponentially decaying field, compares well with the measured data. The magnetic field above the mirror was calibrated using an additional constant offset field, added perpendicular to the direction of the mirror field. Fitting the splitting as a function of the offset field gives the value for the field at the surface of the mirror $B_0=5.3\pm 0.9$ mT/A, which agrees with simple Biot-Savart calculations.

The authors thank Frans Spaepen, Steve Peil, Joe Tien, David Osier, and Steve Shepard for help in fabrication. This work was supported by National Science Foundation (NSF) Grant No. DMR-94-00396 and NSF Grant No. PHY-9312572. MD acknowledges support from the Clare Booth Luce Fellowship, KSJ from the AT&T/Lucent Technologies Ph.D. Fellowship, and JHT from the Fannie and John Hertz Foundation.

- ¹C. S. Adams, M. Sigel, and J. Mlynek, Phys. Rep. **240**, 143 (1994) and references therein.
- ²C. R. Ekstrom, D. W. Keith, and D. E. Pritchard, Appl. Phys. B: Photophys. Laser Chem. **54**, 369 (1992).
- ³A. L. Migdall, J. V. Prodan, W. D. Phillips, T. H. Bergeman, and H. J. Metcalf, Phys. Rev. Lett. **54**, 2596 (1985).
- ⁴W. G. Kaenders, F. Lison, I. Muller, A. Richter, R. Wynands, and D. Meschede, Phys. Rev. A **54**, 5067 (1996).
- ⁵G. I. Opat, S. J. Wark, and A. Cimmino, Appl. Phys. B: Photophys. Laser Chem. **54**, 396 (1992).
- ⁶A. I. Sidorov, R. J. McLean, W. J. Rowlands, D. C. Lau, J. E. Murphy, M. Walkiewicz, G. I. Opat, and P. Hannaford, Quantum Semiclass. Opt. **8**, 713 (1996).
- ⁷T. M. Roach, H. Abele, M. G. Boshier, H. L. Grossman, K. P. Zetie, and E. A. Hinds, Phys. Rev. Lett. **75**, 629 (1995).
- ⁸I. G. Hughes, P. A. Barton, T. M. Roach, and E. A. Hinds, J. Phys. B **30**, 2119 (1997).
- ⁹J. D. Weinstein and K. G. Libbrecht, Phys. Rev. A **52**, 4004 (1995).
- ¹⁰We present a detailed study of atomic deflection using time-dependent potentials in a separate report: K. S. Johnson, M. Drndić, J. H. Thywissen, G. Zabow, R. M. Westervelt, and M. Prentiss (to be published).
- ¹¹*American Institute of Physics Handbook*, edited by D. E. Gray (McGraw-Hill, New York, 1982).
- ¹²*Materials at Low Temperatures*, edited by R. P. Reed and A. F. Clark (American Society for Metals, Metals Park, OH, 1983).
- ¹³We can control this coefficient by controlling the profile of individual wires in the array.
- ¹⁴*Electroplating Engineering Handbook*, edited by L. J. Durney (Van Nostrand Reinhold, New York, 1984).
- ¹⁵For a description of the He^* beam setup see J. Lawall and M. Prentiss, Phys. Rev. Lett. **72**, 993 (1994).